Available online at www.sciencedirect.com
SCIENCE DIRECT®

Chemical Physics Letters 383 (2004) 11–15

CHEMICAL
PHYSICS
LETTERS

www.elsevier.com/locate/cplett

Organic donor/acceptor heterojunction photovoltaic devices based on zinc phthalocyanine and a liquid crystalline perylene diimide

Jung Yong Kim [a,*], Allen J. Bard [b]

[a] *Department of Chemical and Biomolecular Engineering, KAIST, 373-1 Kusong, Yusong, Taejon 305-701, Republic of Korea*
[b] *Department of Chemistry and Biochemistry, The University of Texas at Austin, Austin, TX 78712, USA*

Received 24 September 2003; in final form 30 October 2003

Abstract

An organic photovoltaic cell was fabricated, with the configuration ITO/zinc phthalocyanine (ZnPc)/*N*,*N*′-diheptyl-3,4,9,10-perylenebiscarboximide (PTCDI-C7) (PTCDI)/Ga:In. PTCDI is a liquid crystal and acts as an electron acceptor organic material while ZnPc corresponds to a donor. The cell performance under illumination was examined with different organic layer thickness. A cell incorporating 25 nm thick organic layers showed a short circuit photocurrent (I_{SC}) of 1.6 mA/cm^2, an open circuit photovoltage (V_{OC}) of 0.6 V, and a fill factor (FF) of 0.4 with white Xe light illumination (wavelength $\geqslant$400 nm) with an intensity of 100 mW/cm^2.
© 2003 Elsevier B.V. All rights reserved.

1. Introduction

Organic semiconductors can conduct charges due to partial delocalization or charge hopping through the molecules that are coupled by relatively weak van der Waals forces [1,2]. Cells based on these kinds of materials have been of interest as photovoltaic (PV) and light emitting devices (LED), field effect transistors and memories [3–7]. A number of organic-based PV cells, including organic/inorganic hybrid configurations, have been investigated [8–10]. Typical electron donor materials used in these devices are metal (Zn, Cu, Cd, Pd) porphyrins and phthalocyanines, poly(3-hexyl thiophene), and poly(2-methoxy-5-(2-ethyl)-hexyloxy-*p*-phenylenevinylene) (M EH-PPV). Representative electron acceptors are perylene diimide, PPV with cyano groups (CN-PPV), C_{60}, TiO_2, and CdSe [11–15]. In this study we use *N*,*N*′-diheptyl-3,4,9,10-perylenetetracarboxylicdiimide (PTCDI-C7) as the electron acceptor and zinc phthalocyanine (ZnPc) as the electron donor to fabricate a donor/acceptor (D/A) heterojunction (HJ) PV cell with the configuration ITO/ZnPc/PTCDI-C7/Ga:In (Fig. 1). The proposed device incorporates a liquid crystalline (LC) PTCDI-C7 dye with a long chain–C_7H_{15} hydrocarbon moiety bound to the nitrogen in the imide group. This compound is useful because it is one of few n-type materials and, in addition, self-assembles in thin film due to the LC character in a similar manner to other perylene diimides recently discussed by Gregg, LeBlanc and coworkers [16]. This can make the transport of charges faster and reduce recombination in a PV device. In addition, we used a low melting temperature Ga:In eutectic cathode for this cell, as has been used in LED devices [17]. This material is convenient, because it allows a very simple method of contact formation. Cells of this general type have been recently reviewed [18].

2. Experimental

2.1. Materials

3,4,9,10-perylenetetracarbonate dianhydride (PTC DA), heptylamine, imidazole, tetrabutylammonium hexafluorophosphate ($TBAPF_6$), and ZnPc were purchased from Aldrich Chemical Co. ZnPc was purified by

---

[*] Corresponding author. Fax: +82-42-869-3910.
E-mail address: jykim@kaist.ac.kr (J.Y. Kim).

0009-2614/$ - see front matter © 2003 Elsevier B.V. All rights reserved.
doi:10.1016/j.cplett.2003.10.132

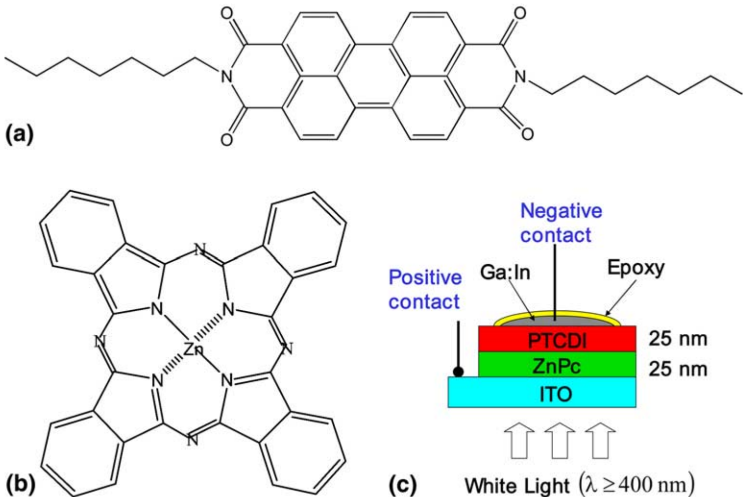

Fig. 1. Structures of: (a) PTCDI; (b) ZnPc; and (c) device configuration.

precipitation in H_2SO_4. Ga:In (75.5:24.5 wt%, mp 15.7 °C) eutectic was obtained from Alfa Aesar.

2.2. Synthesis

N,N′-diheptyl-3,4,9,10-perylenebiscarboximide (PTC DI-C7) was synthesized by condensation of PTCDA with heptylamine, and purified by chromatography with chloroform eluent [19]. ^{1}H NMR(400 MHz/CDCl$_3$): δ (ppm vs. TMS) = 8.7–8.6 (8H from the perylene ring), 4.2 (4H from N–CH_2–), 1.7 (4H from N–CH$_2$–CH_2–), 1.3 (16H from –(CH_2)$_4$–CH$_3$), 0.9 (6H from –CH_3). Differential scanning calorimetry (DSC) (with a scan rate of 5 °C/min): crystal up to 214 °C (36 J/g); the first LC during 214–387 °C (33 J/g); the second LC during 387–403 °C (12 J/g); isotropic phase after 403 °C. Thermogravimetric analysis (TGA) (scan rate of 10 °C/min): PTCDI-C7 is thermally stable up to approximately 410 °C, decomposing at higher temperatures. The decomposition temperature for 20% and 80% weight loss are 455 °C and 560 °C, respectively. Furthermore, *N,N′*-dioctadecyl-3,4,9,10-perylenebiscarboximide (PTCDI-C18) was synthesized by the same method. ^{1}H NMR(400 MHz/CDCl$_3$): δ (ppm vs. TMS) = 8.7–8.6 (8H from the perylene ring), 4.2 (4H from N–CH_2–), 1.7 (4H from N–CH$_2$–CH_2–), 1.3 (60H from –(CH_2)$_{15}$–CH$_3$), 0.9 (6H from –CH_3). Mass spectra (CI+): Mass = 895.635188, Calc. Mass = 895.635285.

2.3. Device fabrication

ZnPc and PTCDI-C7 were evaporated sequentially on ITO glass in a Denton DV 502 Vacuum Chamber at a deposition rate of 0.2–0.5 nm/s. Ga:In eutectic contacts (ca. 2 mm diameter) were printed on the top of the organic films using a syringe and a thin copper wire was inserted into the Ga:In contact [17]. The contact was then covered with 5 min epoxy cement. The illuminated active area in the cell was 3.1 mm^2.

2.4. Characterization

White Xe light (150 W, Oriel) that irradiated the cell had an intensity of 100 mW/cm^2, where a UV filter was used to cut off wavelengths below 400 nm. Current-voltage characteristics were measured with either an electrochemical workstation (Model 660, CHI) or an electrometer (Model 6517, Keithley). Absorption spectra were obtained with a Milton Roy Spectronic 300 Array. Fluorescence spectra were investigated with a Fluorolog-3 Spectroflurometer (ISA-Jobin Yovon Hariba, Edison). Atomic force microscopy was used to check the thickness of film by scanning a scratched area with the tip. ^{1}H NMR spectra were measured at 400 MHz with a Bruker Avance-400 instrument. Thermal behavior was studied by using DSC-2010 and TGA-2050 (TA). X-ray diffraction (XRD) measurements (RIGAKU, Cu Kα radiation) were performed to check the ordering-state for the evaporated thin film on ITO glass at room temperature.

3. Results and discussion

Fig. 1 shows the structures of materials used and the schematic configuration of the PV device. The PTCDI-C7 shows liquid crystalline behavior over 214–403 °C because of the aliphatic group attached to the imide moiety; this was confirmed by DSC. This compound is sufficiently soluble in chloroform to allow a chromatographic method for purification. The room-temperature liquid state Ga:In eutectic used as a cathode has a low work function, 4.12 eV [20], and makes good contact to organic films by printing methods.

Fig. 2 shows the XRD patterns for the evaporated thin films on ITO glass at room temperature: (a) PTCDI-C7, (b) ZnPc and (c) PTCDI-C7/ZnPc with each layer thickness of 100 nm. As shown in this figure, the peaks at $2\theta = 4.50$, and 6.87 represents that PTCDI-C7 and ZnPc are polycrystalline films with orderings of 1.96 and 1.28 nm, respectively, based on the Bragg's law of $\lambda = 2d \cdot \sin\theta(\lambda = 0.154 \text{ nm})$. Especially, the stronger and sharper peak at $2\theta = 4.50$ tells that the PTCDI-C7 film with LC characters has a better organized structure than does the ZnPc with no LC phase.

Cyclic voltammetry was first used to study the electrochemical behavior of the film materials. Fig. 3 shows a cyclic voltammogram (CV) for a spin-coated PTCDI-C18 film (thickness about 150 nm) on ITO glass in a 0.1 M $TBAPF_6$/acetonitrile solution with a Ag/AgCl reference electrode and Pt counter electrode. To obtain this CV, we used PTCDI-C18 instead of PTCDI-C7, because PTCDI-C18 shows a better film-forming property due to the longer aliphatic groups and, more importantly, PTCDI-C18 is not soluble in acetonitrile, while PTCDI-C7 is. While the aliphatic side groups affect the melting point, solubility, and film-forming properties, they exert a negligible effect on both the electrochemical oxidation/reduction potentials and the optical properties (absorbance and fluorescence), which depend on the core structure and the π-conjugation. Thus PTCDI-C18 represents a good model for PTCDI-C7 for obtaining the redox potentials. The CV in Fig. 3 does not represent an ideal thin film CV behavior, probably because of the thickness of the film where the charge transport rate governs the wave shape. However the reduction half-wave potential ($E_{1/2}$) of the PTCDI-C18 film, about −0.7 V vs. Ag/AgCl, is a reasonable measure of the relevant vacant orbital in the compound. This is equiv-

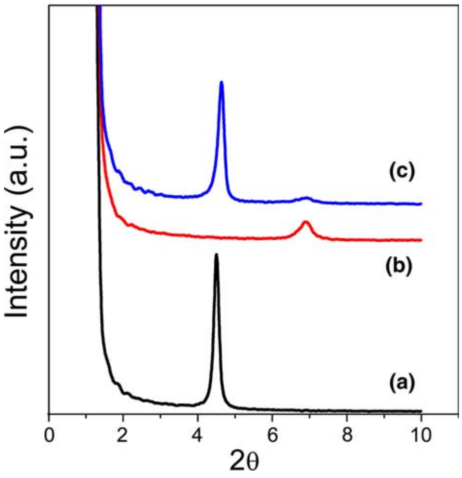

Fig. 2. XRD pattern of evaporated films on ITO glass: (a) PTCDI-C7, 100 nm; (b) ZnPc, 100 nm; and (c) PTCDI-C7/ZnPc, 100:100 nm.

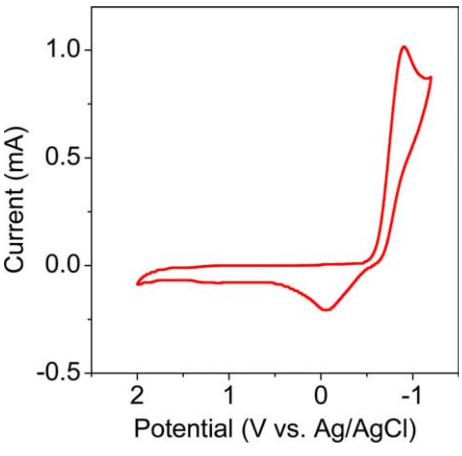

Fig. 3. CV for spin-coated PTCDI-C18 film (working electrode) on ITO glass in 0.1 M $TBAPF_6$/acetonitrile with Ag/AgCl reference electrode and platinum counter electrode at scan rate of 100 mV/s.

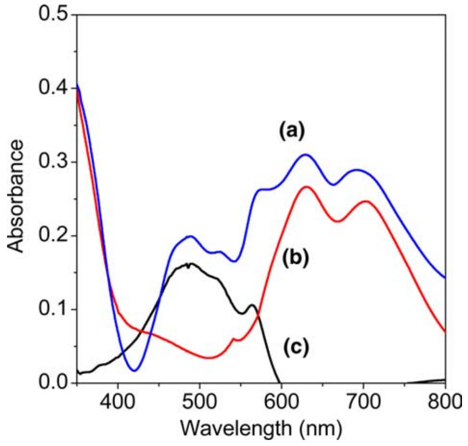

Fig. 4. Absorption spectra for evaporated films on ITO glass referenced to bare ITO glass: (a) ZnPc:PTCDI, 25:25 nm; (b) ZnPc, 25 nm; and (c) PTCDI, 25 nm.

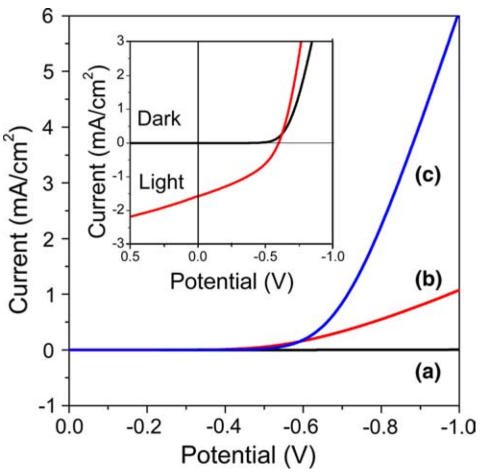

Fig. 5. Dark current potential characteristics for ZnPc: PTCDI-C7 films of: (a) 100:100 nm; (b) 50 nm:50 nm; and (c) 25 nm: 25 nm. Inset: Current-potential characteristics for the device with configuration as ITO/ZnPc (25 nm)/PTCDI-C7 (25 nm)/Ga:In under irradiation with Xe light (>400 nm), 100 mW/cm^2.

Table 1
The short circuit photocurrent, open circuit photovoltage, fill factor (FF) and absorbance for several dual layer or single layer devices with different organic film-thicknesses

System	Thickness (nm)	I_{SC} (mA/cm^2)	V_{OC} (V)	FF[a]	Absorbance[b]
ZnPc:PTCDI-C7	100: 100	0.40	0.60	0.22	1.0–0.9
	50: 50	1.40	0.60	0.30	0.6–0.5
	25: 25	1.58	0.60	0.40	0.3–0.2
ZnPc	25	0.09	0.31	0.31	0.3–0.2
PTCDI-C7	25	0.02	0.11	0.30	0.2–0.1

Xe light (wavelength $\geqslant$ 400 nm) intensity, 100 mW/cm^2.

[a] FF = $I_{PP}V_{PP}/I_{SC}V_{OC}$ (where, subscript 'pp' denotes peak power).

[b] Absorbance is the maximum value in the visible range (400–800 nm).

alent to about −4 eV on the vacuum energy scale, taking −4.5 eV vs. vacuum level corresponding to 0 V vs. NHE in aqueous solution and 0.197 V vs. NHE as 0 V vs. Ag/AgCl. This level is only approximate because the film CV is not nernstian and is obtained in a different solvent. However, it provides a useful rough estimate for the location of the lowest unoccupied molecular orbital (LUMO) of the PTCDI films. The highest occupied molecular orbital (HOMO) can be estimated from the LUMO energy and the optical band gap, which can be obtained from the absorption spectra edge. As shown in Fig. 4, optical band edge is about 600 nm, which is equivalent to a ca. 2.1 eV optical band gap. This places the HOMO at about −6.1 eV vs. vacuum level. The PTCDI-C18 dissolved in chloroform shows an optical band gap in solution state (as opposed to the solid-film state) of about 2.3 eV, slightly larger than that of the spin-coated film. For ZnPc, the LUMO and the HOMO are about −3.8 and −5.4 eV, respectively, as calculated from the oxidation (0.68 V vs. SCE) and the reduction (−0.90 V vs. SCE) potentials [21–23]. Fig. 4 also shows the absorption spectra for a 25 nm film of ZnPc and a ZnPc/PTCDI-C7 (25 nm each) dual layer. As shown in this figure, by combining ZnPc and PTCDI-C7 films, we can harvest across the whole visible range.

Fig. 5 shows the dark current–potential (*I–V*) characteristics for the PV device with the configuration as ITO/ZnPc/PTCDI-C7/Ga:In, with several different thicknesses of each film layer (ZnPc/PTCDI): (a) 100:100 nm, (b) 50:50 nm, and (c) 25:25 nm. We define forward bias for a negative potential is applied to the Ga:In contact. When the thickness of each layer was 100 nm, the dark current was about 0.03–3.53 μA at −0.6 to −1 V, respectively. Under these conditions, when white light with an intensity of 100 mW/cm^2 (wavelength $\geqslant$400 nm), irradiated the device, the I_{SC}, V_{OC}, and FF was 0.40 mA/cm^2, −0.6 V, and 0.22, respectively (see Table 1). The poor $FF = 0.22$ can be attributed to a high series resistance of the cell because of the film thickness. We also checked a cell with the reverse configuration, ITO/PTCDI-C7/ZnPc/Ga:In. The resulting parameters were much worse: $I_{SC} = 0.8$ μA/cm^2, $V_{OC} = +0.069$ V, $FF = 0.25$. Note that the open circuit potential showed the opposite polarity compared with the ITO/ZnPc/PTCDI-C7/Ga:In configuration. In any event, at this film thickness the performance was very poor, although the absorbance in this cell was 0.9–1 (∼90% of incident light absorbed). One can trade off absorbance for lower film resistance by reducing the film thickness. For ITO/ZnPc:PTCDI-C7/Ga:In at 50:50 nm, the dark current was 0.16–1.07 mA/cm^2 at −0.6 to −1 V, suggesting significant reduction in resistance. I_{SC}, and *FF* were improved to 1.40 mA/cm^2, and 0.30, respectively (see Table 1), but the FF is still very low. For ITO/ZnPc:PTCDI-C7/Ga:In at 25:25 nm, significantly better performance was found (see, inset), with $I_{SC} = 1.58$ mA/cm^2, $V_{OC} = 0.6$ V, and $FF = 0.40$. The improvement can be attributed to the efficient separation of electron-hole pairs and the ready movement of free charges to each electrode contact (i.e., a short diffusional length), even though the harvesting of incident photons is more reduced.

4. Conclusions

A simple HJ PV device with the printed Ga:In contact based on the liquid crystalline PTCDI-C7 and ZnPc shows promising results for an organic thin film device, including a relatively high open circuit photovoltage (600 mV). Future studies will include the detail comparison of the evaporated LC PTCDI film and the non-LC one in both the pristine and the thermal-treated states, and focus on improvement of the geometry of the HJ to increase the FF and absorbance.

Acknowledgements

Support of this project by the National Science Foundation (CHE 0202136) and the Robert A. Welch Foundation is greatly appreciated.

References

[1] H. Meier, Organic Semiconductors: Dark and Photoconductivity of Solids, Verlag Chemie, 1974.

[2] J. Simon, J.-J. Andre, Molecular Semiconductors, Springer Verlag, 1985.
[3] C.-Y. Liu, A.J. Bard, Acc. Chem. Res. 32 (1999) 235.
[4] F.G. Gao, A.J. Bard, Chem. Mat. 14 (2002) 3465.
[5] G. Horowitz, Adv. Mat. 10 (1998) 365.
[6] C.-Y. Liu, H. Pan, M.A. Fox, A.J. Bard, Science 261 (1993) 897.
[7] J. Nelson, Curr. Opin. Mat. Sci. 6 (2002) 87.
[8] C.W. Tang, Appl. Phy. Lett. 48 (1986) 183.
[9] L. Schmidt-Mende, A. Fechtenkötter, K. Müllen, E. Moons, R.H. Friend, J.D. MacKenzie, Science 293 (2001) 1119.
[10] W.U. Huynh, J.J. Dittmer, A.P. Alivisatos, Science 295 (2002) 2425.
[11] B.A. Gregg, M.A. Fox, A.J. Bard, J. Am. Chem. Soc. 111 (1989) 3024.
[12] B.A. Gregg, Chem. Phy. Lett. 258 (1996) 376.
[13] G. Yu, A.J. Heeger, J. Appl. Phys. 78 (1995) 4510.
[14] G. Yu, J. Gao, J.C. Hummelen, F. Wudl, A.J. Heeger, Science 270 (1995) 1789.
[15] U. Bach, D. Lupo, P. Comte, J.E. Moser, F. Weissörtel, J. Salbeck, H. Spreitzer, M. Grätzel, Nature 395 (1998) 583.
[16] S.-G. Liu, G. Sui, R.A. Cormier, R.M. Leblanc, B.A. Gregg, J. Phys. Chem. B 106 (2002) 1307.
[17] F.G. Gao, A.J. Bard, Chem. Mat. 14 (2002) 3465.
[18] B.A. Gregg, J. Phys. Chem. B 107 (2003) 4688.
[19] C.W. Struijk, A.B. Sieval, J.E.J. Dakhorst, M. van Dijk, P. Kimkes, R.B.M. Koehorst, H. Donker, T.J. Schaafsma, S.J. Picken, A.M. van de Craats, J.M. Warman, H. Zuilhof, E.J.R. Sudhölter, J. Am. Chem. Soc. 122 (2000) 11057.
[20] V.V. Emets, B.B. Damaskin, J. Electroanal. Chem. 491 (2000) 30.
[21] A. Wolberg, J. Manassen, J. Am. Chem. Soc. 92 (1970) 2982.
[22] J. Manassen, A. Bar-Ilan, J. Catal. 17 (1970) 86.
[23] A.B.P. Lever, J.P. Wilshire, Can. J. Chem. 54 (1976) 2514.